



Molecular Crystals and Liquid Crystals Incorporating Nonlinear Optics

Publication details, including instructions for authors and subscription information:

<http://www.tandfonline.com/loi/gmcl17>

Investigation of the Nematic-Isotropic Biphase in Thermotropic Main Chain Polymers. Homogeneity of the Pure Nematic and Isotropic Phases. Part I: Microscopy and Fractionation

J. F. D'alless^a, P. Sixou^a, A. Blumstein^b & R. B. Blumstein^b

^a Laboratoire de Physique de la Matière Condensée, Nice, Cedex, U.A. C.N.R.S. 190, Faculté des Sciences-Parc Valrose, 06034, (France)

^b Polymer Science Program, Department of Chemistry, University of Lowell, Lowell, MA, 01854
Version of record first published: 19 Dec 2006.

To cite this article: J. F. D'alless, P. Sixou, A. Blumstein & R. B. Blumstein (1988): Investigation of the Nematic-Isotropic Biphase in Thermotropic Main Chain Polymers. Homogeneity of the Pure Nematic and Isotropic Phases. Part I: Microscopy and Fractionation, *Molecular Crystals and Liquid Crystals Incorporating Nonlinear Optics*, 157:1, 229-251

To link to this article: <http://dx.doi.org/10.1080/00268948808080235>

PLEASE SCROLL DOWN FOR ARTICLE

Full terms and conditions of use: <http://www.tandfonline.com/page/terms-and-conditions>

This article may be used for research, teaching, and private study purposes. Any substantial or systematic reproduction, redistribution, reselling, loan, sub-licensing, systematic supply, or distribution in any form to anyone is expressly forbidden.

The publisher does not give any warranty express or implied or make any representation that the contents will be complete or accurate or up to date. The accuracy of any instructions, formulae, and drug doses should be independently verified with primary sources. The publisher shall not be liable for any loss, actions, claims, proceedings, demand, or costs or damages whatsoever or howsoever caused arising directly or indirectly in connection with or arising out of the use of this material.

INVESTIGATION OF THE NEMATIC-ISOTROPIC BIPHASE IN
THERMOTROPIC MAIN CHAIN POLYMERS. HOMOGENEITY OF
THE PURE NEMATIC AND ISOTROPIC PHASES.
PART I: MICROSCOPY AND FRACTIONATION.

J.F. d'ALLEST, P. SIXOU

Laboratoire de Physique de la Matière Condensée,
U.A. C.N.R.S. 190, Faculté des Sciences-Parc Valrose
06034 Nice Cedex (France)

A. BLUMSTEIN AND R.B. BLUMSTEIN

Polymer Science Program, Department of Chemistry,
University of Lowell, Lowell, MA 01854

Abstract Two moderately low melting main chain nematic polymers with flexible spacers are investigated (spacers $(CH_2)_7$ and $(CH_2)_{10}$). Isothermal evolution in the N+I biphasic is considered as an orientational ordering stage followed by macroscopic demixing of the N and I domains and homogenization of their respective chain length distributions. Segregation according to chain length is studied by means of polarizing microscopy and fractionation. A method for delineation of equilibrium biphasic width is presented, for masses ranging up to $\overline{M}_n=37,000$. Evolution of the gross morphology of the pure nematic and solid phases as a function of thermal history in the biphasic is illustrated.

INTRODUCTION

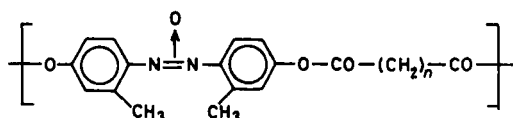
Under the phase rule, thermotropic mixtures of nematogens are expected to display a nematic-isotropic (N+I) biphasic in which the composition of the two coexisting phases can be determined from consideration of phase equilibria.

Experimentally, however, binary mixtures of low molecular mass nematics at best exhibit a very narrow biphasic gap^{1,2,3}. Moreover, in a ternary system composed of p-oxybenzoate oligomers, the selective partitioning of components between the nematic and isotropic phases

predicted by lattice theory is not confirmed by experiment and compositions of the coexisting phases are found to be identical within experimental error⁴.

On the other hand, in main chain polymeric liquid crystals (PLCs), polydispersity of chain lengths brings about a polydispersity of isotropization temperatures that appears as a broad N+I biphasic characteristic of such systems^{5,6,7,8}. It is our purpose here to discuss molecular segregation in the biphasic of flexible main chain nematic polystyres as well as the impact of this segregation on the homogeneity and morphology of the ensuing isotropic, nematic and solid phases.

In a previous investigation of the homologous series of PLCs formed by regularly alternating mesogens and



flexible spacer groups, selective partitioning of chain lengths in the N+I biphasic was reported for the case of spacer length $n=10$. The longest chains were preferentially transferred into the anisotropic component^{7,9}. In addition, preliminary DSC¹⁰ and NMR experiments⁹ suggest that molecular morphology and homogeneity of the pure nematic phase and subsequently, of the solid polymer may be determined by sample thermal history in the precursor N+I biphasic. This question merits systematic study and will be addressed here in some detail. If the pure N phase is indeed formed of metastable "domains" (defined as regions segregated by chain length and, hence, level of order), investigation of their stability and kinetics of formation will shed light on fundamental problems of

textures, morphology and rheological properties in main chain PLCs.

Accurate determination of biphasic width and temperature dependence of the nematic fraction f_N is also essential: presence of a minor isotropic component can be expected to influence rheological behavior, orientation dynamics and level of orientational order of the mesophase, as well as the mechanical properties of the solid. For example, in fibers extruded from the mesophase melt, optimum mechanical strength is not developed until extrusion temperatures are below the I/N transition of the shortest component, that is below the N+I biphasic^{8,11}. Similarly, the nematic order parameter achieves its maximum value only following complete disappearance of a residual I component⁹. The minor I component is also found to be rate determining in the kinetics of alignment of a nematic polymer subjected to a magnetic field¹².

In the present series of papers we report a detailed investigation of the N+I biphasic for two polymers belonging to the above homologous series, with spacer length $n=10$ and 7 (labelled polymers DDA9 and AZA9, respectively). Chain segregation and demixing of isotropic and anisotropic domains in the biphasic are followed under various conditions of thermal history. Kinetics of subsequent remixing in the pure N and the pure I phase, as well as homogeneity of the pure N or I phase are investigated by a combination of polarizing optical microscopy, differential scanning calorimetry and broad line NMR. Finally, biphasic width is delineated under conditions approaching thermodynamic equilibrium.

The polymers chosen for this study have moderately low transition temperatures (melting and isotropization are in

the vicinity of 100 to 150°C respectively) and can be maintained in the N+I biphasic for extended periods of time without chain degradation or reorganization. The biphasic appears solely as a result of polydispersity of chain lengths without the complicating factors due to inhomogeneity in composition, as would be the case in a copolymer. Consequently, polymers DDA9 and AZA9 will provide a model system for study of phase equilibria and kinetics of phase separation in main chain thermotropic nematics PLCs.

Study of polarizing microscopy and fractionation is reported in the first paper of this series. Results from DSC and NMR investigation are discussed in the second and third papers. Polarizing microscopy allows observation of the evolution of gross morphology of segregated domains in the solid, N, and N+I phases as a function of sample molecular mass, spacer parity and thermal history.

EXPERIMENTAL SECTION

Sample synthesis and characterization were as described previously^{7,13}. The polydispersed samples are designated as DDA9Mx or AZA9Mx, where Mx represents the number average molecular mass. Polydispersity index varied in the range 1.2-1.7. Some sharp fractions (dispersity index ≤ 1.1) were also used (see below).

Fractionation in the N+I biphasic was done as described in¹⁰ by equilibrating the sample in sealed tubes blanketed with nitrogen. The separated I and N components were analyzed by gel permeation chromatography (GPC) as described elsewhere⁸, with calibration performed using models, oligomers and sharp fractions of DDA9 and AZA9.

Biphase fractionation experiments were carried out in the temperature range of 100-160°C. GPC performed before and after annealing shows that sample degradation can be considered as negligible below 160°C and care was taken to avoid lengthy annealing above that temperature. In addition, a fresh sample was used for every annealing experiment above 150°C.

Polarizing microscopy experiments were carried out on an Olympus instrument equipped with a Mettler FP52 Hot Stage and FP5 temperature programmer as well as a photomultiplier (PM) for thermal optical analysis. Sample thickness was approximately 10 μm . In a typical annealing experiment in the biphase, the sample was degassed and homogenized for about 30 minutes at approximately 15°C past the complete isotropization temperature. It was then brought to the segregation temperature T_s , annealed at T_s for a time t_s , quenched on a cold plate and again heated to 15 degrees beyond complete isotropization (scanning rate of 5°C/min).

Extended annealing in the biphase results in demixing of macroscopic N and I domains. Upon cooling from the biphase, these domains remain demixed and clearly distinguishable, in the N and in the solid phase. These components are subsequently referred to as FN and FI, formerly nematic and isotropic components of the biphase, respectively. The temperature of beginning $(T_1)_{FI}$ and end $(T_2)_{FI}$ of isotropization of FI component and the temperature of beginning $(T_1)_{FN}$ and end $(T_2)_{FN}$ of isotropization of FN components were recorded. Results are most accurate if $(T_1)_{FI}$ is recorded as the temperature at which PM signal begins to drop rather than from visual

observation.

TABLE I Definition of Symbols

T_1, T_2 and ΔT

Beginning and end of the biphasic, and biphasic width, respectively, of the "original" (or "untreated") sample; i.e. a sample that has not been isothermally treated within the biphasic.

$(T_1)_{FI}, (T_2)_{FI}$ and $(\Delta T)_{FI}$;

$(T_1)_{FN}, (T_2)_{FN}$ and $(\Delta T)_{FN}$

Refer to the corresponding temperatures in the FI and FN components of the biphasic.

$(\Delta T)_{eq}$

Biphasic width on equilibrium demixing (as described in the text section).

RESULTS AND DISCUSSION

Isothermal evolution in the biphasic is decomposed, somewhat arbitrarily, into two stages: i) I/N phase separation, which occurs via normal nucleation and growth (orientational and conformational ordering); ii) growth and coalescence of the I and N domains till equilibrium (macroscopic) demixing, concomitant with homogenization of chain length distribution within these respective domains.

Segregation experiments within the N+I biphasic were carried out by means of polarizing microscopy on four polydisperse samples: DDA9M5,200, DDA9M20,000, AZA9M6,000 and AZA9M37,000. The partially or completely demixed

biphase was quenched and the isotropization temperatures of FI and FN components were measured upon reheating beyond the pure N phase. Isotropization of the FI component was followed by isotropization of the FN component, as expected, since T_{NI} increases with increasing chain length^{7,14}.

VISUAL OBSERVATION

The segregation phenomenon can be followed visually as illustrated on Figs. 1,2,3 and 4. In the case of DDA9, phase separation in the biphase begins either as a dispersion of isotropic droplets within a continuous N phase or as a dispersion of nematic droplets within a continuous I phase, depending on the location of the annealing temperature T_g (Fig. 1). Droplet size increases with

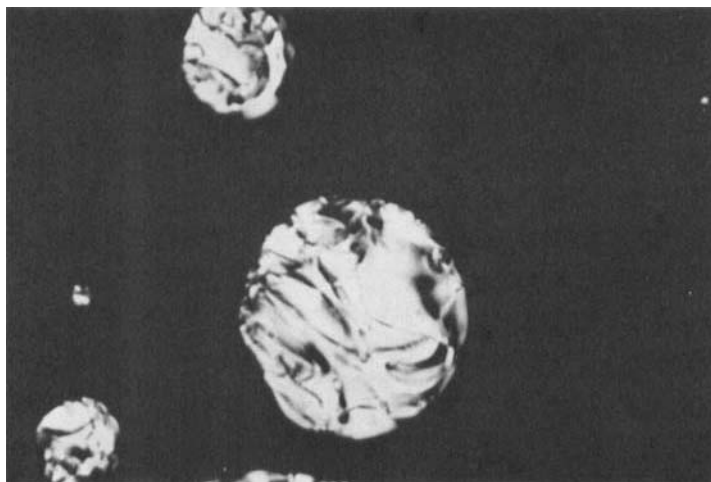


FIGURE 1. Nematic droplets in DDA9M5,500 at 144°C
Magnification x 825.

increasing annealing time t_g and the droplets may eventually coalesce. Droplets are also observed in AZA9M37,000, but not in AZA9M6,000, where shapes such as shown in Fig. 3 are displayed.

Equilibrium Demixing

Following initial phase separation, the I and N domains grow in size until demixing is achieved. This state of equilibrium is characterized somewhat arbitrarily by stabilization of PM signal intensity, domain size and boundaries. Figs. 2 a-d show photomicrographs of sample DDA9M5,500 annealed for 12 hours at $T_g=136^\circ\text{C}$, (PM signal stabilizes after 4 hours). Fig. 2a shows the brightly birefringent FN component and the dark brown FI globules in the solid phase. On subsequent reheating, DSC scans display two cold crystallization peaks, two T_{KN} and two T_{NI} peaks, one for each of the former components of the biphasic (see following paper). Figs. 2b-d illustrate the sequential isotropization of the demixed FI and FN domains. The interface between these domains remains virtually intact upon isotropization. The N phase remaining within the $(\Delta T)_{FI}$ interval is uniformly dispersed in an isotropic matrix (Figs. 2b and c). Conversely, the I phase develops within the $(\Delta T)_{FN}$ range as uniformly dispersed droplets in a nematic matrix (Fig. 2d). This implies a uniform distribution of chain lengths within the I and N domains, on the dimensional scale of microscopy.

When the sample is held for about 20 min. in the I phase (at 135°C past $(T_2)_{FN}$) to erase thermal history and cooled back to the pure N phase at $5^\circ/\text{min.}$, a somewhat blurred mirror image of the previous FN/FI morphology is recovered. These memory effects and lack of homogeneity of



FIGURE 2A. Photomicrograph of DDA9M5,500 quenched to room temperature after 12 hours of annealing at 136°C. Magnification x 165.

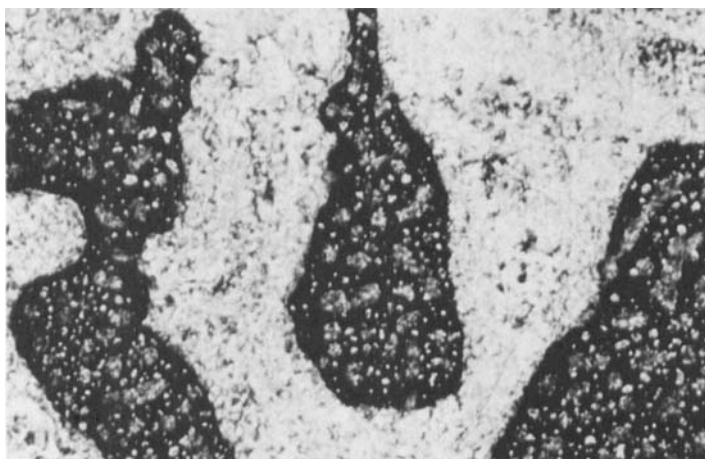


FIGURE 2B. Isotropization of FI component (124°C).



FIGURE 2C. Isotropization of FI component (136°C).

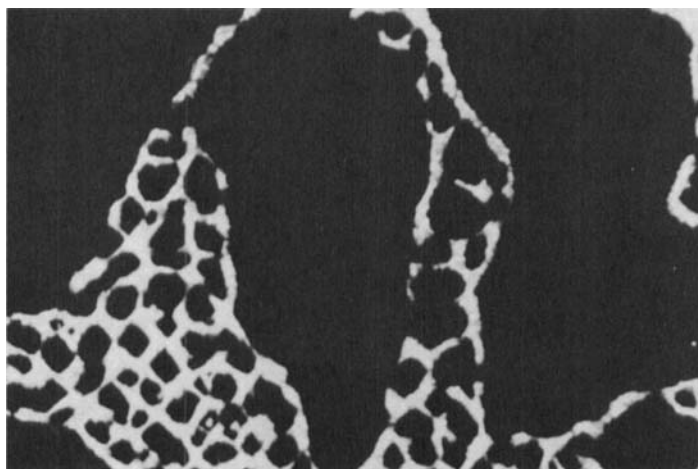


FIGURE 2D. Isotropization of FN component (150°C).

the pure I phase are illustrated by numerous experiments (see Parts II and III).

Figs. 3a and b show photomicrographs of sample AZA9M6,000 following annealing for 15 hours (complete demixing) at $T_g=144^\circ\text{C}$, with the I component forming the continuous phase. The shape of the dispersed N domains contrasts strikingly with the nematic droplets observed in sample DDA9. Quenching preserves the FN and FI domains, as in DDA9, but with smaller contrast in birefringence. Complete demixing is suggested by absence of interfacial zone and stability of domain boundaries as the sample is reheated through the pure N phase and the biphase. Chain lengths appear to be uniformly distributed within FN and FI components, a conclusion based on the homogeneous progression of isotropization.

Incomplete Demixing

Fig. 4 illustrates incomplete demixing in sample DDA9M5,500 at $T_g=144^\circ\text{C}$, where the I component forms the continuous phase. Annealing time was 12 hours, but this was not sufficient to stabilize the PM signal which continued to drop steadily, suggesting incomplete demixing. The more birefringent FN phase appears "marbled" with darker streaks of FI component (4a). Isotropization progresses from FI through a broad boundary region common to both components (figs. 4 b and c). This implies a gradient of molecular mass distribution across the boundary.

BIPHASE WIDTH (ΔT)_{eq}

On Figs. 5 and 6 are plotted isotropization temperatures of FI and FN components as a function of segregation temperature T_g . Data are shown for DDA9M20,000 and AZA9M6,000, with DDA9M5,500 and AZA9M37,000 giving similar

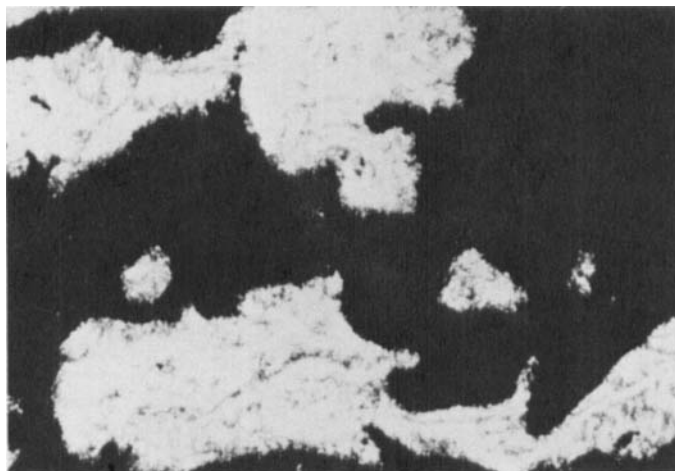


FIGURE 3A. AZA9M6,000 following 12 hours of annealing at $T_g = 144^\circ\text{C}$. Isotropization of FI component (137°C). Magnification $\times 165$.

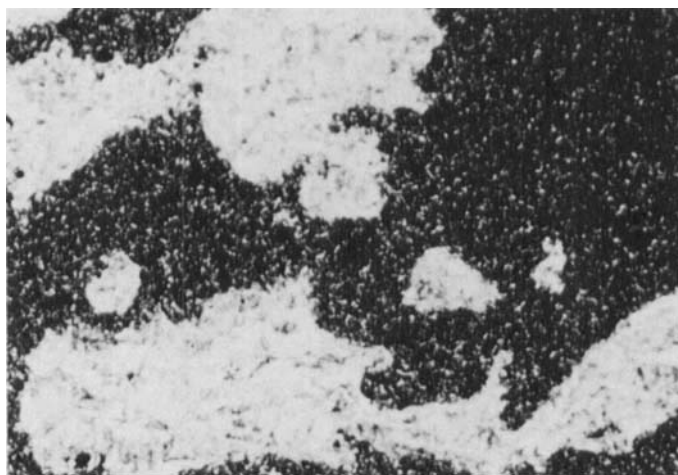


FIGURE 3B. Isotropization of FN component (146°C).

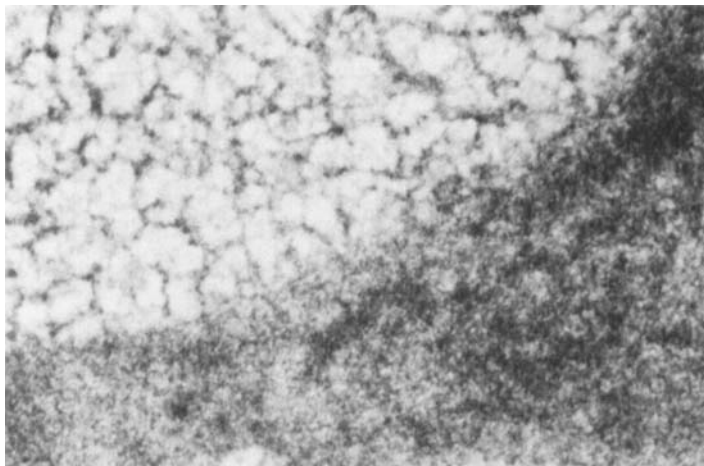


FIGURE 4A. Photomicrograph of DDA9M5,500 quenched to room temperature following incomplete demixing. Magnification $\times 165$.

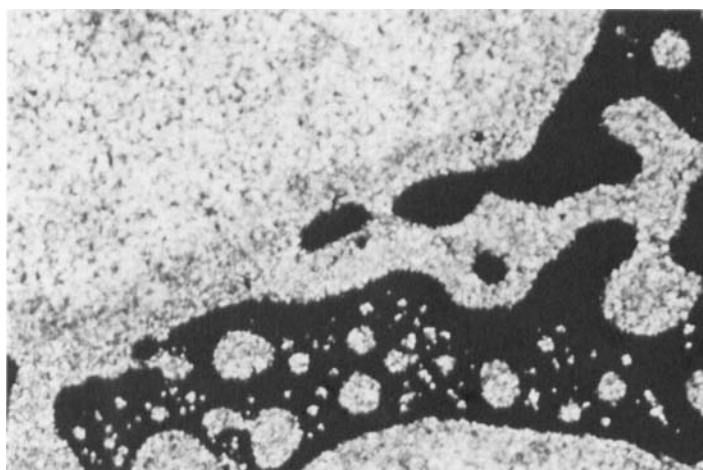


FIGURE 4B. Progression of isotropization across the boundary region (145°C).

results. Annealing times at each value of T_g were adjusted to give complete demixing, as apparent from the sequential isotropization of the FI and FN components. Transition temperatures and widths are recorded in Tables II and III and compared with the values for the original polymer where the various chain lengths are assumed to be homogeneously distributed.

Molecular segregation according to chain length is clearly illustrated. Isotropization temperatures of both components increase with increasing T_g , as their average molecular weight increases. As polydispersity of the FN component decreases with increasing T_g , the value of

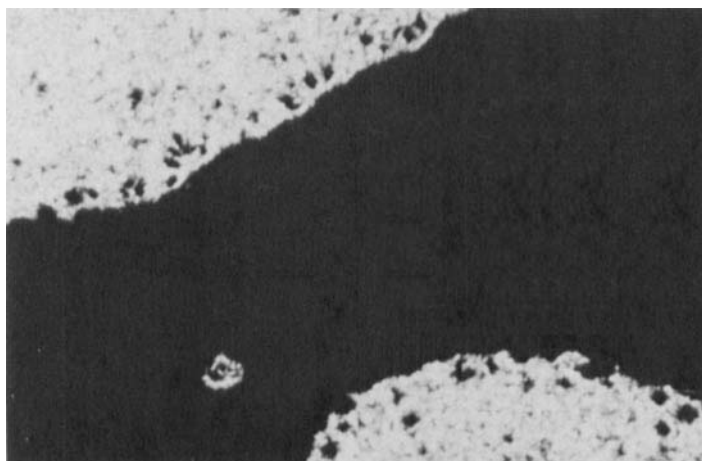


FIGURE 4C. Progression of isotropization across the boundary region (147°C).

$(\Delta T)_{FN}$ decreases. On the other hand, an increase in the polydispersity of the FI component with T_g is not coupled with an increase of $(\Delta T)_{FI}$. This can be readily understood

by considering the molecular mass dependence of isotropization temperatures (Fig. 8).

Biphase width (ΔT)_{eq} in the completely demixed sample (i.e. interval between lowest $(T_1)_{FI}$ and highest $(T_2)_{FN}$) is much broader than ΔT in the unannealed polymer, with $(T_1)_{FI}$ significantly lower than T_1 and $(T_2)_{FN}$ higher than T_2 . Trailing of a residual I component well below T_1 was also observed when the temperature dependence of the nematic fraction f_N was determined from proton NMR spectra upon very slow cooling from the I phase^{7,8}. Demixing within the biphase enables the shortest chains to concentrate on cooling and to isotropize close to their "equilibrium" temperatures, relatively unaffected by dilution with other chains. On the other hand when an unannealed sample is heated, the shortest chains are more nearly molecularly dispersed and thus may either isotropize above their "equilibrium" temperatures or form I domains that are too small to be detected under our sensitivity constraints.

In samples such as the higher molecular mass DDA9 shown on Fig. 5, which cannot be aligned in a NMR spectrometer¹⁵, biphase width cannot be measured by NMR. Microscopy, on the other hand, seems to provide a reliable way to determine "equilibrium" biphase width in even the highest molecular mass samples that we have studied ($\bar{M}_n=37,000$). A measure of the relative amounts of the I and N components can also be derived from their volume fractions as measured by microscopy (Fig. 7). In order to measure "equilibrium" transition temperatures as a function of chain length, annealing experiments were carried out on a series of DDA9 and AZA9 fractions (polydispersity

TABLE II Isotropization temperatures and biphas width of DDA9M20,000
as a function of T_s .

T_s ($^{\circ}\text{C}$)	FI Component		$(\Delta T)_{FI}$	FN Component		$(\Delta T)_{FN}$
	$(T_1)_{FI}$	$(T_2)_{FI}$		$(T_1)_{FN}$	$(T_2)_{FN}$	
149				151.9	165.3	13.4
150	-	152	-	153	166	13
151	133	155.5	22.5	155.7	166.4	10.7
152	136.2	159	22.8	159.3	166.6	7.3
154	138.5	161	22.5	161	166.7	5.7
156	140.8	161.7	20.9	161.9	167.4	5.5
158	141.5	162.2	20.7	162.4	167.5	5.1
160	143.5	163.4	19.9	164	168	4
162	144.2	164	19.8	165	168.5	3.5
163	146	165.4	19.4	166	168.9	2.9
164	151	165	14	-	-	
original polymer	151.2	165.5	14.3			

TABLE III Isotropization temperatures and biphas width of AZA9M6,000 as a function of T_s .

T_s ($^{\circ}\text{C}$)	FI Component		FN Component		$(\Delta T)_{\text{FI}}$	$(T_1)_{\text{FI}}$	$(T_2)_{\text{FI}}$	$(T_1)_{\text{FN}}$	$(T_2)_{\text{FN}}$	$(\Delta T)_{\text{FN}}$
	$(T_1)_{\text{FI}}$	$(T_2)_{\text{FI}}$								
140	135	144.3			1.3			146	154.1	8.1
141	135.8	144.9			9.1			146.8	154.5	7.7
142	137.2	146.4			9.2			147.4	154.9	7.5
143	138.5	147.3			8.8			147.9	151.1	7.2
144	139.3	148.2			8.9			148.8	155.3	6.5
146	140.3	149.5			9.2			150.1	155.5	5.4
148	141	150.8			9.8			151.7	155.7	4
149	141.6	151.4			9.8			152.4	155.7	3.3
150	142.2	151.9			9.8			152.8	155.7	2.9
152	142.5	152.6			10.8			-	-	-
original polymer	142.7	151.9			9.2			-	-	-

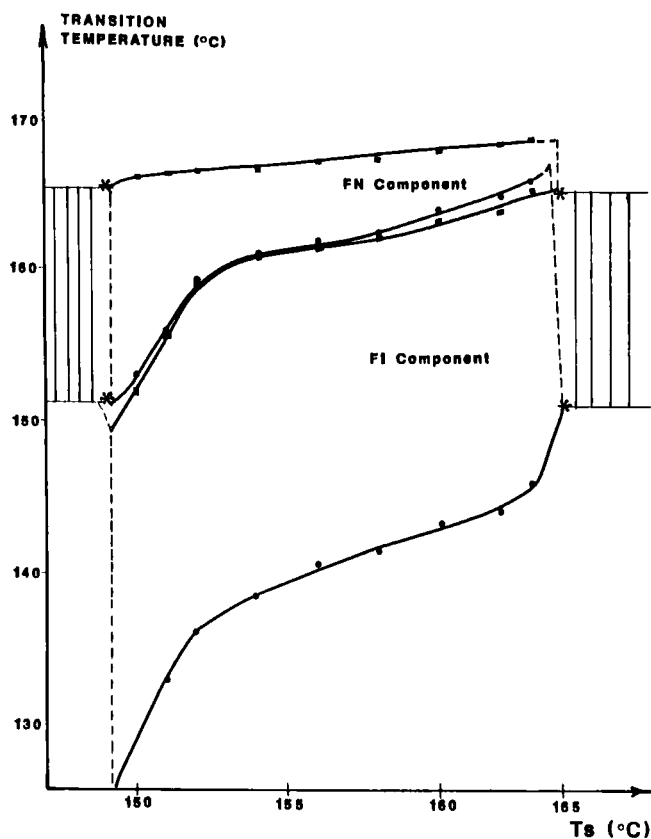


FIGURE 5. Isotropization temperatures of DDA9M20,000 as a function of annealing temperature T_s (complete demixing). Beginning (●) and end (■) of isotropization of FI and FN components. Points represented by * illustrate apparent discontinuity in biphasic width.

index ≤ 1.1). On Fig. 8 is plotted the mass dependence of transition temperatures and $(\Delta T)_{eq}$. The biphasic in DDA9 fractions is about two times wider than in AZA9. Note that

a similar difference between odd and even spacer lengths is observed for the remainder of this homologous series ($n=4-14$). The biphasic gap with n =odd spacers is intermediate between standard LMLCs and n =even spacers, possibly because the latter polymers display a cybotactic nematic¹⁴ organization.

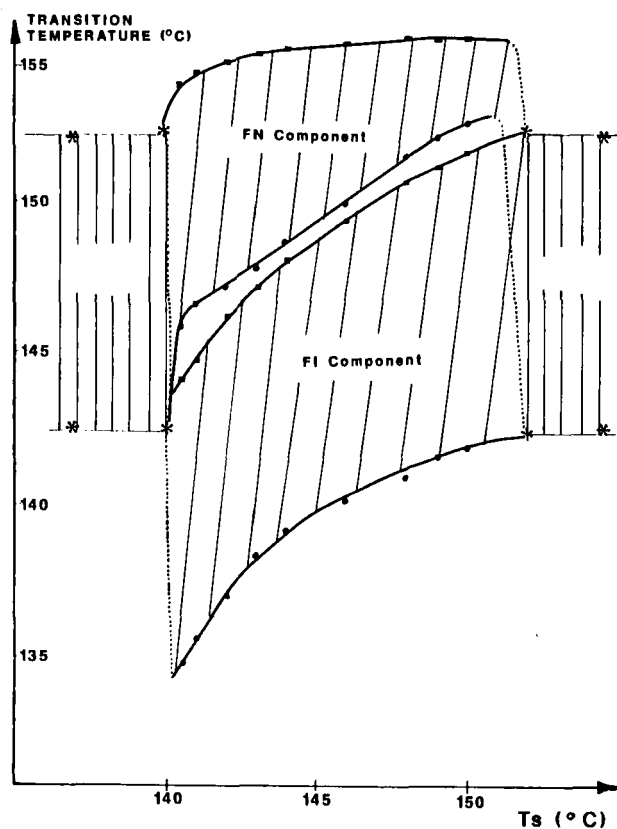


FIGURE 6. Isotropization temperatures of AZA9M6,000 as a function of T_g (complete demixing) symbols as for Fig. 5.

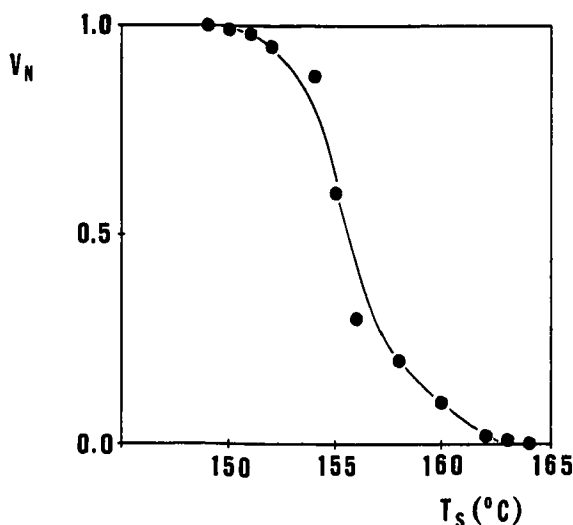


FIGURE 7. Volume fraction of the nematic component in DDA9M20,000 as a function of T_s .

FRACTIONATION

Table IV shows fractionation results for two DDA9 samples fractionated as described in ref.¹⁰. From the data presented above one can expect the molecular mass of both the I and N components to increase with increasing annealing temperature T_s . These expectations are qualitatively fulfilled and substantial fractionation is observed even in the case of DDA9M3,300, a sample with low polydispersity. Fractionation experiments on a sample of AZA9 were inconclusive, probably because a sharp meniscus between the I and N components failed to develop. Regions similar to shapes illustrated on Fig.3, but 5-10mm in size, appeared instead.

Similar fractionation experiments were performed by

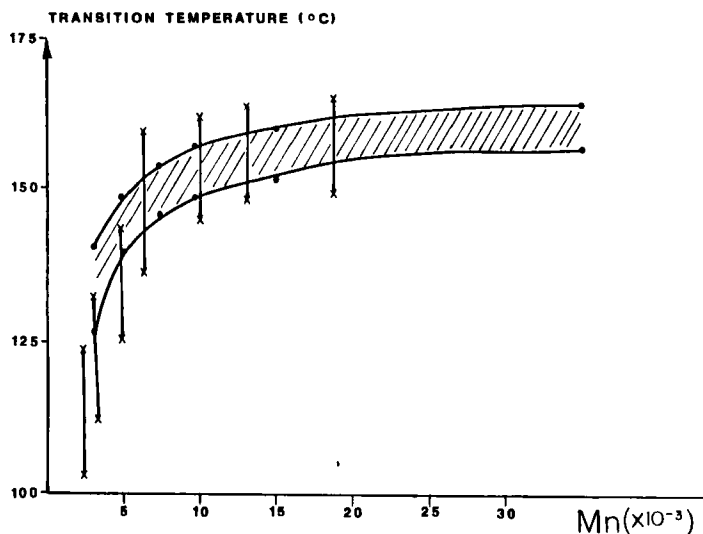


FIGURE 8. Molecular weight dependence of biphasic width $(\Delta T)_{eq}$ for AZA9 (●) and DDA9 (X) fractions.

Ballauff and Flory⁴ on ternary mixtures of p-oxybenzoate oligomers. As mentioned previously, compositions of the coexisting I and N components were identical within experimental error, in marked departure of lattice theory predictions of selective chain length partitioning. The authors interpreted their results by assuming that orientational ordering propagates rapidly and supersedes compositional equilibration. The latter would require mass transport on a macroscopic scale and migration of chains across the I/N boundary may be very slow under the minute gradient of chemical potential that prevails as a result of the low values of isotropization entropies in p-oxybenzoate oligomers.

TABLE IV Fractionation of DDA9 samples.

Sample	$T_g (\pm 0.3^\circ\text{C})$	f_N	Component	\overline{M}_n	$\overline{M}_w/\overline{M}_n$
DDA9M5,200			original	5200	1.5
	133	0.45	I	3000	1.8
			N	5600	1.4
	138	0.23	I	3800	1.7
			N	8900	1.4
DDA9M3,000			original	3300	1.2
	137	0.52	I	2900	1.2
			N	3300	1.2
	140	0.33	I	2700	1.2

SUMMARY

When considering migration of chains following the initial orientational ordering stage one must distinguish:

i) equilibration of chain length distributions between the I and N components, which involves transport across phase boundaries; ii) homogenization of chain length distributions within the respective boundaries of the I and N components. A discussion of this point will be presented in Part III where the phase separation process will be considered on a molecular level.

Polarizing microscopy experiments clearly illustrate the impact of molecular segregation in the I+N biphasic on the morphology of the I, N and solid phases. "Equilibrium" biphasic width can be accurately delineated even in high molecular mass samples where the biphasic cannot be monitored by methods such as NMR. Complete demixing of the I and N components produces a macrodomain morphology with sharply defined FN/FI boundaries and uniform distribution of chain

lengths within boundaries. Upon incomplete demixing intermediate chain lengths are seen to accumulate in a broad interfacial zone. Kinetics of homogenization of the pure I and N phases will be discussed in parts II and III.

ACKNOWLEDGEMENT

This work was supported in part by National Science Foundation Grant DMR 8600029.

REFERENCES

1. J.S. Dave and M.J.S. Dewar, J. Chem. Soc., 4616 (1954); ibid., 4305 (1955).
2. H. Kelker and R. Hatz, Handbook of Liquid Crystals Verlag Chemie, Weinheim, 1980), pp. 372-383.
3. M. Ballauf, D.Wu, P.J. Flory and E.V. Barrett II, Ber. Bunsenges. Phys. Chem., 88, 524 (1984).
4. M. Ballauf and P.J. Flory, ibid., 530
5. W.R. Krigbaum, A. Ciferri, J. Preston, J. Asrar and H. Toriumi, Mol. Cryst. Liq. Cryst., 76, (1981).
6. W.R. Krigbaum, T. Ishikawa, J. Watanabe, H. Toriumi, K. Kubotane and J. Preston, J. Polym. Sci., Polym. Phys. Ed., 21, 1851 (1983).
7. R.B. Blumstein, E.M. Stickles, M.M. Gauthier, A. Blumstein and F. Volino, Macromolecules, 17, 177 (1984).
8. R.B. Blumstein, O. Thomas, M.M. Gauthier, J. Asrar and A. Blumstein, Polymeric Liquid Crystals, A. Blumstein Ed. (Plenum Press, New York, 1985) p. 249.
9. F. Volino, J.M. Allonneau, A.M. Giroud, R.B. Blumstein E.M. Stickles and A. Blumstein, Mol. Cryst. Liq. Cryst. (Letters), 102, 21 (1984).
10. J.F. d'Allest, P.P. Wu, A. Blumstein and R.B. Blumstein Mol. Cryst. Liq. Cryst. (Letters), 3, (3-4), 103 (1986).
11. O. Thomas, Ph.D. Dissertation, Department of Chemistry University of Lowell, 1984.
12. J.S. Moore and S.I. Stupp, Macromolecules, 20, 282 (1987).
13. A. Blumstein and O. Thomas, Macromolecules, 15, 1264 (1982).
14. A. Blumstein, S. Vilasagar, S. Ponrathnam, S.B. Clough and R.B. Blumstein, J. Polym. Sci., Polym. Phys. Ed., 20, 877 (1982).
15. A.F. Martins, J.F. Ferreira, F. Volino, A. Blumstein and R.B. Blumstein, Macromolecules, 16, 279 (1983).